JOURNAL OF BACTERIOLOGY, Feb. 2008, p. 1054–1063 Vol. 190, No. 3
0021-9193/08/$08.00+0 doi:10.1128/JB.01523-07

Identification of Type 3 Fimbriae in Uropathogenic *Escherichia coli* Reveals a Role in Biofilm Formation▽

Cheryl-Lynn Y. Ong,[1] Glen C. Ulett,[1] Amanda N. Mabbett,[1] Scott A. Beatson,[1] Richard I. Webb,[2] Wayne Monaghan,[3] Graeme R. Nimmo,[3] David F. Looke,[4] Alastair G. McEwan,[1] and Mark A. Schembri[1]*

School of Molecular and Microbial Sciences[1] and Centre for Microscopy and Microanalysis,[2] University of Queensland, Brisbane, Australia, and Queensland Health Pathology Service[3] and Infection Management Services, Princess Alexandra Hospital, Brisbane, Australia[4]

Received 21 September 2007/Accepted 17 November 2007

Catheter-associated urinary tract infection (CAUTI) is the most common nosocomial infection in the United States. Uropathogenic *Escherichia coli* (UPEC), the most common cause of CAUTI, can form biofilms on indwelling catheters. Here, we identify and characterize novel factors that affect biofilm formation by UPEC strains that cause CAUTI. Sixty-five CAUTI UPEC isolates were characterized for phenotypic markers of urovirulence, including agglutination and biofilm formation. One isolate, *E. coli* MS2027, was uniquely proficient at biofilm growth despite the absence of adhesins known to promote this phenotype. Mini-Tn*5* mutagenesis of *E. coli* MS2027 identified several mutants with altered biofilm growth. Mutants containing insertions in genes involved in O antigen synthesis (*rmlC* and *manB*) and capsule synthesis (*kpsM*) possessed enhanced biofilm phenotypes. Three independent mutants deficient in biofilm growth contained an insertion in a gene locus homologous to the type 3 chaperone-usher class fimbrial genes of *Klebsiella pneumoniae*. These type 3 fimbrial genes (*mrkABCDF*), which were located on a conjugative plasmid, were cloned from *E. coli* MS2027 and could complement the biofilm-deficient transconjugants when reintroduced on a plasmid. Primers targeting the *mrkB* chaperone-encoding gene revealed its presence in CAUTI strains of *Citrobacter koseri*, *Citrobacter freundii*, *Klebsiella pneumoniae*, and *Klebsiella oxytoca*. All of these *mrkB*-positive strains caused type 3 fimbria-specific agglutination of tannic acid-treated red blood cells. This is the first description of type 3 fimbriae in *E. coli*, *C. koseri*, and *C. freundii*. Our data suggest that type 3 fimbriae may contribute to biofilm formation by different gram-negative nosocomial pathogens.

Catheter-associated urinary tract infection (CAUTI) is the most common nosocomial infection in the United States, where it accounts for approximately 40% of all nosocomial infections (49). Although CAUTI is usually asymptomatic, it is a frequent cause of bacteremia and infected patients can also experience fever, acute pyelonephritis, and death (59). The risk of bacteriuria following urethral catheterization is estimated to be 5 to 10% per day (60). Most patients with indwelling urinary catheters for 30 days or longer develop bacteriuria (49).

Nosocomial CAUTI is caused by a range of gram-negative and gram-positive organisms, including *Escherichia coli*, *Proteus mirabilis*, *Pseudomonas aeruginosa*, *Providencia stuartii*, *Staphylococcus epidermidis*, and *Enterococcus faecalis* (60). These infections are often polymicrobial and can last from several days to months (29). *E. coli* is one of the most common organisms isolated from the urine of CAUTI patients. Like uropathogenic *E. coli* (UPEC) strains that cause cystitis and pyelonephritis, CAUTI *E. coli* strains possess a range of virulence factors, including adhesins (e.g., P and type 1 fimbriae) and toxins (e.g., hemolysin), and express certain O antigen and capsule (K) types (29). Adherence is important for the colonization of the urinary tract, and the best-characterized adhesins of UPEC are P and type 1 fimbriae from the chaperone-usher subclass. P fimbriae are associated most strongly with pyelonephritis and contribute to the establishment of bacteriuria by binding to the α-D-galactopyranosyl-(1-4)-β-D-galactopyranoside receptor epitope in the globoseries of glycolipids (22, 27). Type 1 fimbriae are produced by most *E. coli* strains and contribute to the colonization of the bladder by binding to α-D-mannosylated proteins, such as uroplakins (62). Both P and type 1 fimbriae recognize their receptor targets by virtue of organelle tip-located adhesins, namely PapG and FimH, respectively (25).

CAUTI results from the growth of bacterial biofilms on the inner surface of the urinary catheter. Biofilm formation promotes encrustation and protects bacteria from the hydrodynamic forces of urine flow, host defenses, and antibiotics (58). The removal and replacement of the infected catheter is often the only option for patients with symptomatic CAUTI. Treatment with antibiotics is thought to merely postpone the onset of bacteriuria and may result in the emergence of resistant bacteria in the patient and in the medical unit (58). Indeed, in intensive care units, CAUTI can be caused by bacteria that are resistant to all known antibiotics (34).

The mechanisms by which CAUTI *E. coli* strains adhere to and form biofilms on the surfaces of urinary catheters have not been well described. Several different factors have been associated with biofilm formation by *E. coli*, including type 1 and F9 fimbriae, flagella, curli, and antigen 43 (24, 29, 37, 38, 53). Here we examined in detail the biofilm-forming properties of

* Corresponding author. Mailing address: School of Molecular and Microbial Sciences, University of Queensland, Brisbane QLD 4072, Australia. Phone: 61 7 3365 3306. Fax: 61 7 3365 4699. E-mail: m.schembri@uq.edu.au.

▽ Published ahead of print on 30 November 2007.

TABLE 1. Bacterial strains and plasmids

Strains/plasmids	Description	Reference
E. coli strains		
MS427	K-12 MG1655 *flu*	39
MS528	K-12 MG1655 *fim flu*	25
MS661	MS427*recA*::*tet*	39
MS1219	*E. coli* S17-1 + pUT(mini-Tn*5kan*)	30
MS1355	Rifampin resistant MS2027	This study
MS1520	*E. coli* DH5α containing pCO10	This study
MS1486	MS2027 transconjugant P4-6E (*mrkD*::Tn*5kan*)	This study
MS1488	MS2027 transconjugant P20-5B (*mrkB*::Tn*5kan*)	This study
MS1489	MS2027 transconjugant P20-11A (*mrkA*::Tn*5kan*)	This study
MS1502	MS2027 transconjugant P17-9H (*rmlC*::Tn*5kan*)	This study
MS1505	MS2027 transconjugant P20-11B (*manB*::Tn*5kan*)	This study
MS1506	MS2027 transconjugant P22-3H (*kpsM*::Tn*5kan*)	This study
MS1998	MS528 + pCO12	This study
MS2000	MS528 + pBR322 (no insert)	This study
MS2001	MS1486 + pCO12	This study
MS2003	MS1486 + pBR322 (no insert)	This study
MS2004	MS1488 + pCO12	This study
MS2006	MS1488 + pBR322 (no insert)	This study
MS2007	MS1505 + pCO12	This study
MS2009	MS1505 + pBR322 (no insert)	This study
MS2027	*E. coli* CAUTI isolate	This study
Plasmids		
pCO10	Plasmid from MS1486 (*mrkD*::Tn*5kan*)	This study
pCO12	*mrkABCDF* amplified from *E. coli* MS2027 with primers 871 and 872 and ligated into EcoRV site of pBR322	This study
pBR322	Cloning vector	63

the *E. coli* strain MS2027, which was isolated from a patient with nosocomial CAUTI. Genes associated with the formation of O antigen, capsule, and type 3 fimbriae were found to influence biofilm growth. This is the first report to describe the production and functional role of type 3 fimbriae in *E. coli*.

MATERIALS AND METHODS

Bacterial strains, plasmids, and growth conditions. The strains and plasmids used in this study are described in Table 1. Clinical UTI isolates were obtained from urine samples of patients at the Princess Alexandra Hospital (Brisbane, Australia). The *E. coli* reference (ECOR) collection was obtained from the STEC Center, Michigan State University. *E. coli* MS427 (MG1655 *flu*) and *E. coli* MS528 (MG1655 *fim flu*) have previously been described (23, 37). *E. coli* MS661 is *E. coli* MS427 *recA*::*tet*. *E. coli* MS1355 is a spontaneous rifampin-resistant mutant of *E. coli* MS2027. Cells were routinely grown at 37°C on solid or in liquid Luria-Bertani (LB) medium supplemented with appropriate antibiotics unless otherwise stated. M9 minimal medium consisted of 42 mM Na_2HPO_4, 22 mM KH_2O_4, 9 mM NaCl, 18 mM NH_4Cl, 1 mM $MgSO_4$, 0.1 mM $CaCl_2$, and 0.2% glucose (41) supplemented with appropriate antibiotics.

DNA manipulations and genetic techniques. Plasmid DNA was isolated by using the QIAprep Spin Miniprep kit (Qiagen, Australia). Restriction endonucleases were used according to the manufacturer's specifications (New England Biolabs). Chromosomal DNA was purified by using the GenomicPrep cell and tissue DNA isolation kit (Amersham Pharmacia Biotech, Inc., Australia). PCR was performed by using the Expand Long Template PCR system (for amplification of the *mrk* gene cluster) or *Taq* polymerase (for screening assays) according to the manufacturer's instructions (Roche, Australia). DNA sequencing was performed by the Australian Genome Research Facility. The *mrk* gene cluster was amplified from *E. coli* MS2027 by PCR using primers 871 (5′-CGC GCGATATCGCAGCATAACCGAACAAATG) and 872 (5′-CCGGGGATAT CTAAATTTTCTGCGGCAAACC). The PCR product was digested with EcoRV and ligated to the EcoRV-digested plasmid pBR322 to construct plasmid pCO12.

Phenotypic assays. Type 1 fimbria expression was assayed by the ability of bacterial cells to cause mannose-sensitive (MS) agglutination of yeast (*Saccharomyces cerevisiae*) cells on glass slides (46). Bacterial strains were grown overnight as shaking cultures in LB broth. Those strains with negative results by this assay were retested after three successive rounds of 48 h of static growth in LB broth. Mannose-resistant (MR) agglutination was assessed as described previously (15). Briefly, a 5% suspension (10 μl) of human type A red blood cells (RBC) washed in phosphate-buffered saline (PBS) was mixed with a 10-μl bacterial suspension on glass slides in the presence and in the absence of D-mannose. The bacterial suspension was prepared by transferring cells from a freshly grown LB agar colony into 50 μl PBS. Bacterial agglutination of tannic acid-treated human RBC (MR/K agglutination) was performed as described previously (10). Curli production was detected by the ability of colonies to stain with Congo red (63).

Transposon mutagenesis. Transposon mutagenesis was performed via filter paper bacterial conjugation (7, 9). An overnight culture of the donor strain was concentrated 10-fold and left to stand at 37°C for 30 min to allow growth of the sex pili. The donor and recipient were then mixed in a ratio of 1:10 and left to incubate on filter paper for 3 to 4 h. The filter paper mixture was then resuspended in LB and plated out on selective antibiotic medium. Colonies confirmed as kanamycin resistant and ampicillin sensitive were tested for biofilm growth in the microtiter assay. Transposon insertion sites of transconjugants with altered biofilm abilities were identified by using inverse PCR as described previously (57). Primers 390 (5′-GGTTCTTTTTGTCAAGACCGACCTGT) and 391 (5′-CAGTCTAGCTATCGTCATGTAAGCCCACT) were used in combination with TaqαI digestion and religation; primers 395 (5′-AAGCTTGCTCAATCA ATCACC) and 465 (5′-CGCCAACTATTGCGATAACA) were used in combination with HhaI digestion and religation.

Biofilm study. Biofilm formation on polyvinyl chloride (PVC) surfaces was monitored by using 96-well microtiter plates (Falcon) essentially as described previously (45). Briefly, cells were grown for 24 h in M9 minimal medium (containing 0.2% glucose) at 37°C, washed to remove unbound cells and stained with crystal violet. The quantification of bound cells was performed by the addition of acetone-ethanol (20:80) and measurement of the dissolved crystal violet at an optical density of 595 nm (OD_{595}). Flow chamber biofilm experiments were performed as described previously (23, 44), with the exception that cells were detected by using BacLight green fluorescent stain (Molecular Probes). Briefly, biofilms were allowed to form on glass surfaces in a multichannel flow system that permitted online monitoring of community structures. Flow cells were inoculated with OD_{600}-standardized pregrown overnight cultures in M9 medium. BacLight green fluorescent stain was used at a concentration of 0.1 mM, according to the manufacturer's instructions. Biofilm development was monitored by confocal scanning laser microscopy at 20 to 24 h after inoculation. All experiments were performed in triplicate.

Scanning electron microscopy (SEM). Cells were grown as described for the biofilm study on polystyrene surfaces, with the exception that the experiment was performed by using a 12-well microtiter plate (Greiner Bio-One) with a polystyrene disc placed at the bottom. The disc was fixed with 3% glutaraldehyde in 0.1 M cacodylate buffer and postfixed with 1% osmium tetroxide in 0.1 M cacodylate buffer. The sample was then infiltrated with glycerol and frozen in liquid nitrogen. The sample was freeze-substituted in 100% ethanol containing a molecular sieve and left at −80°C for 10 h, and then the temperature was increased from −80°C to −20°C over a 10-h period and critical point dried. The sample was then mounted on carbon tabs and sputter coated with platinum 15 mA for 120 s.

Phylogenetic analysis. PCR products obtained from screening for the presence of *mrkB* were sequenced from 36 strains. Sequences were trimmed to obtain 130 nucleotides of high-quality sequence corresponding to the central region of *mrkB* (i.e., nucleotides 179 to 308 of *mrkB* in *K. pneumoniae* MGH78578). Phylogenetic analyses of 36 aligned *mrkB* sequences were carried out by using PHYLIP (8, 12, 16, 20). Consensus trees of bootstrap analyses were prepared by using the consensus network method (8, 12, 16, 20) as implemented by SplitsTree, version 4 (8, 12, 16, 20). Evidence for recombination was assessed by using the pairwise homoplasy index recombination test (8, 12, 16, 20).

Statistical analysis. Differences in comparison of phenotypes from CAUTI *E. coli* and *E. coli* from other UTI syndromes were determined by using a chi-square test for the differences between two groups. Differences in biofilm phenotypes (mean optical density values) were compared by using a *t* test with a linear mixed model; each microtiter plate well was treated as a random effect, and each gene

TABLE 2. Comparison of phenotypes from CAUTI *E. coli* and *E. coli* from other UTIs

Source of isolates	Value for phenotype[a]								
	MS agglutination			MR agglutination			Biofilm		
	No. of isolates (%)	PR	*P*	No. of isolates (%)	PR	*P*	No. of isolates (%)	PR	*P*
CAUTI ($n = 65$)	54 (83)			10 (15%)			40 (62%)		
Pyelonephritis ($n = 26$)	24 (92)	1.11	0.42	13 (50%)	3.33	0.00	4 (15%)	0.24	0.00
Cystitis ($n = 19$)	19 (100)	1.20	0.12	5 (26%)	1.73	0.45	8 (42%)	0.68	0.21
ABU ($n = 57$)	42 (74)	0.89	0.30	14 (25%)	1.67	0.30	24 (42%)	0.68	0.05

[a] Where the prevalence ratios (PR) and *P* values are relative to CAUTI isolates.

modification was treated as a fixed effect. All comparisons were against the values for *E. coli* MS2027. Both analyses were performed by using the statistical analysis program R (36a).

Nucleotide sequence accession numbers. The *mrkB* sequence fragments from 34 strains were deposited in GenBank under accession numbers EU109428 to EU109460. The complete 9.3-kb *mrk* cluster (and adjacent regions) from *E. coli* MS2027 was deposited in GenBank under accession number EU105468.

RESULTS

Biofilm formation by CAUTI *E. coli* strains. Sixty-five CAUTI *E. coli* strains from our UTI collection were examined for the ability to cause MS agglutination of yeast cells, MR agglutination of human RBC, and biofilm formation. These phenotypes were compared to those of strains collected from patients with asymptomatic bacteriuria (ABU), cystitis, and pyelonephritis from the same geographic location (Table 2). Sixty-two percent of the CAUTI *E. coli* strains were positive by the biofilm assay, while 42% of ABU ($P = 0.05$) and 15% of pyelonephritis strains were positive ($P < 0.05$). There was no correlation between biofilm formation and MR agglutination of human RBC. Biofilm analysis of the 65 CAUTI *E. coli* strains revealed a range of phenotypes (Fig. 1). To identify novel factors associated with biofilm formation by CAUTI *E. coli*, we studied strains that exhibited strong biofilm growth for the expression of type 1 fimbriae (by MS agglutination of yeast cells) and curli production (by Congo red staining). *E. coli* MS2027 was identified as a unique strong biofilm former that did not express type 1 fimbriae or curli under the growth conditions employed in this study. We therefore chose *E. coli* MS2027 for an in-depth molecular analysis.

Generation of *E. coli* MS2027 mini-*Tn5* mutants altered in biofilm formation. A collection of approximately 2,000 Km^r transposon insertion mutants were screened for their ability to form biofilms. Two types of biofilm mutants were obtained: (i) mutants displaying an enhanced biofilm phenotype and (ii) mutants displaying a decreased biofilm phenotype. SEM was performed to examine the structure of the biofilms produced by *E. coli* MS2027 and selected mutants representing each phenotype (Fig. 2). The enhanced biofilm growth of *E. coli* MS1502 and *E. coli* MS1506 correlated with a more densely packed arrangement of cells than the growth of *E. coli*

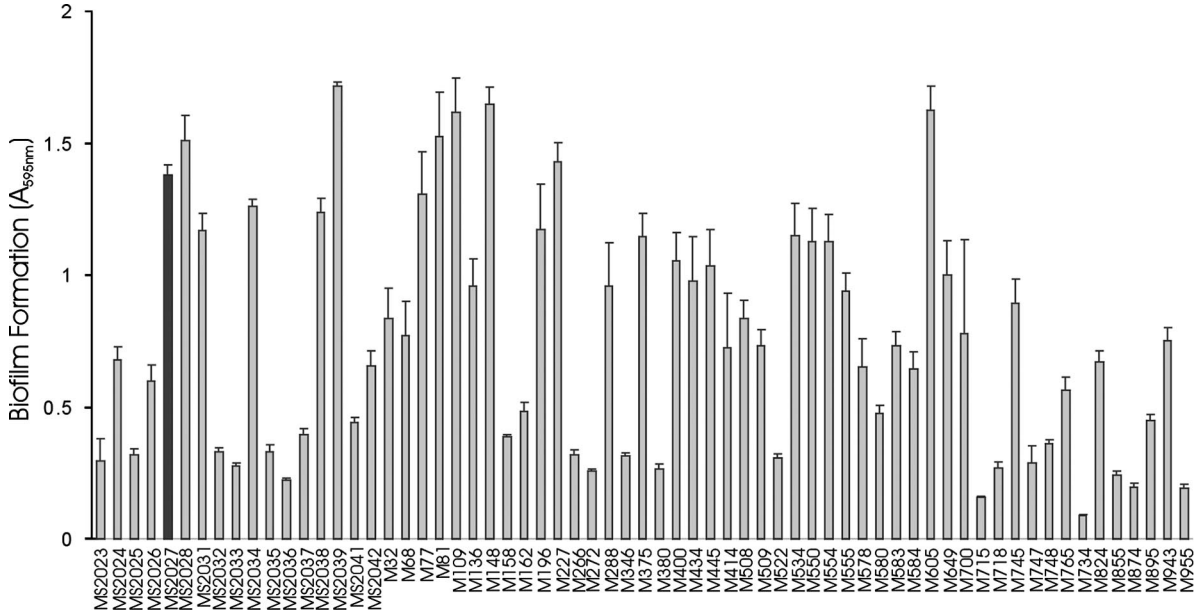

FIG. 1. Biofilm formation by CAUTI *E. coli* strains. Strains were grown at 37°C in PVC microtiter plates containing M9 medium (supplemented with 0.2% glucose) for 16 h under shaking conditions, washed to remove unbound cells, and stained with 0.1% crystal violet. Biofilm formation was quantified by resuspending adhered cells in ethanol-acetate (80:20) and measuring the absorbance at 595 nm. The results are presented as the average of eight individual replicates (± standard deviation [error bars]). An arbitrary cutoff of OD_{595} at 0.5 was used, and strains were scored as either positive or negative for biofilm formation. The black bar highlights *E. coli* MS2027.

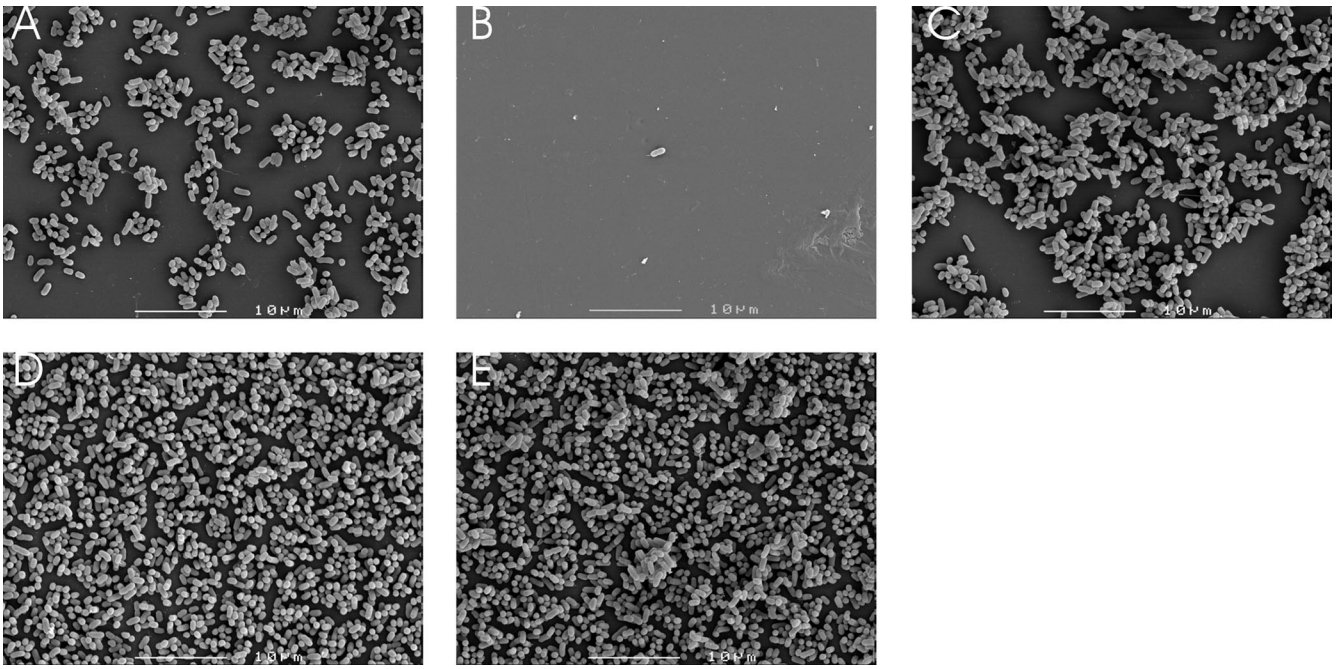

FIG. 2. SEM micrographs depicting the biofilm structures of *E. coli* MS2027 and representative Tn*5* mutants. (A) *E. coli* MS2027, (B) *E. coli* MS1486 (MS2027 *mrkD*::Tn*5kan*), (C) *E. coli* MS2001 (MS1486 complemented with pCO12), (D) MS1502 (MS2027 *rmlC*::Tn*5kan*), and (E) MS1506 (MS2027 *kpsM*::Tn*5kan*). Cells were grown in 12-well microtiter plates (Greiner Bio-One) containing a polystyrene disc placed at the bottom. Following overnight growth, the disc was removed, fixed, stained, and examined by SEM as described in Materials and Methods. Scale bar, 10 μm.

MS2027. In contrast, cells from the biofilm-deficient mutant *E. coli* MS1486 were virtually undetectable. All of the mutants exhibited a growth rate indistinguishable from that of the wild-type strain (data not shown).

The insertion site of each mutant was determined by inverse PCR. The sequencing of the DNA flanking the transposon insertion site for the mutants displaying the enhanced biofilm phenotype (i.e., MS1502, MS1505, and MS1506) revealed that the transposon insertions disrupted genes associated with O antigen or capsule production (Table 3). In the case for the mutants displaying the decreased biofilm phenotype (i.e., MS1486, MS1488, and MS1489), all of the transposon insertions disrupted the same genetic locus, but at different positions. Blast analysis revealed that this genetic locus was homologous to the *mrk* (type 3 fimbriae) genetic locus of *K. pneumoniae* (Table 3). Unlike the *E. coli* MS2027 parent strain, all of these mutants were unable to exhibit MR/K agglutination, a standard assay for monitoring the expression of type 3 fimbriae in *K. pneumoniae*.

TABLE 3. Transposon mutagenesis results for strain *E. coli* MS2027

Strain	Biofilm type	Gene disrupted	Gene function
MS1486	Reduced	*mrkD*	Adhesin of type 3 fimbriae
MS1488	Reduced	*mrkB*	Chaperone of type 3 fimbriae
MS1489	Reduced	*mrkA*	Major subunit of type 3 fimbriae
MS1502	Increased	*rmlC*	dTDP-4-dehydrorhamnose 3,5-epimerase of OAg gene cluster
MS1505	Increased	*manB*	Phosphomannomutase of OAg gene cluster
MS1506	Increased	*kpsM*	Polysialic acid transport protein, membrane component

The *E. coli mrk* gene locus is carried on a conjugative plasmid. *E. coli* MS2027 contains several plasmids, and we suspected that the *mrk* genes were located on one of these. Thus, we attempted to transfer the *mrk* genes (containing Tn*5*-kanamycin) from the Tn*5* mutants MS1486, MS1488, and MS1489 into a tetracycline-resistant *E. coli* MG1655 derivative strain (MS661) via conjugation. Indeed, we were able to obtain kanamycin-resistant *E. coli* MS661 transconjugants using all three Tn*5* mutants by this method. PCR using primers specific for the *mrk* sequence identified previously by inverse PCR demonstrated that the *mrk* genes were located on this conjugative plasmid. The plasmid that originated from *E. coli* MS1486 was designated pCO10.

Characterization of the *E. coli mrk* gene locus. The *mrk* locus was sequenced directly from pCO10 on both DNA strands by primer walking. The sequence of the region disrupted by the Tn*5* insertion was confirmed by PCR and sequencing from the intact plasmid in *E. coli* MS2027 (designated pMS2027). The *mrk* gene cluster contains six open reading frames (ORFs) arranged in the same transcriptional orientation, including genes that encode a putative major subunit protein (*mrkA*) as well as putative chaperone (*mrkB*)-, usher (*mrkC*)-, adhesin (*mrkD*)-, and anchor (*mrkF*)-encoding genes (Fig. 3). The *E. coli mrk* locus does not contain a putative regulator gene (*mrkE*) upstream of *mrkA*, unlike the *K. pneumoniae mrk* locus. Instead, this DNA sequence has a mosaic structure. The nucleotide sequence immediately upstream of *mrkA* is 98%

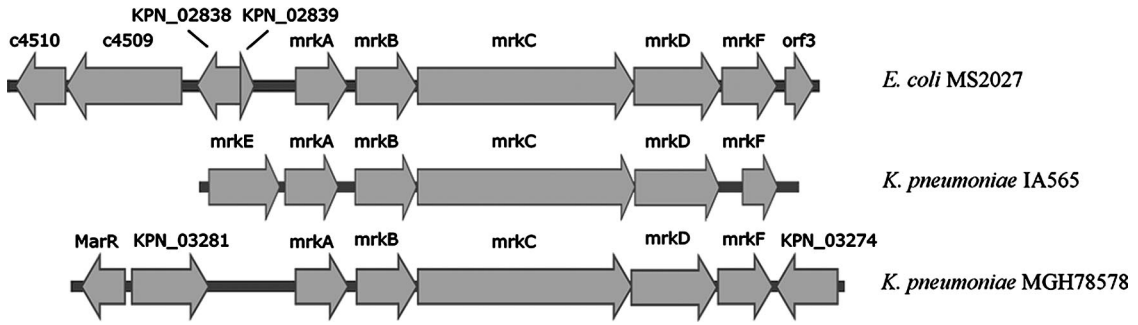

FIG. 3. Physical map of the *mrk* gene cluster and adjacent regions from *E. coli* MS2027, *K. pneumoniae* IA565, and *K. pneumoniae* MGH78578. The *mrk* genes are indicated and include *mrkE* (putative regulatory gene), *mrkA* (major subunit encoding gene), *mrkB* (chaperone encoding gene), *mrkC* (usher encoding gene), *mrkD* (adhesin encoding gene), and *mrkF* (encoding a putative anchor protein). The *mrk* genes from *E. coli* MS2027 and *K. pneumoniae* IA565 are plasmid located, while the *mrk* genes from *K. pneumoniae* MGH78578 are chromosomally located. ORFs adjacent to the *mrk* genes from both *E. coli* MS2027 and *K. pneumoniae* MGH78578 are also shown. *E. coli* MS2027-adjacent ORFs were KPN_02838 (encodes a putative IS*1* transposase from *K. pneumoniae* MGH78578), KPN_02839 (encodes a putative insertion element protein from *K. pneumoniae* MGH78578), *orf3* (encodes a putative cytoplasmic protein), and c4510 and c4509 (encode putative hypothetical proteins from *E. coli* UPEC CFT073). *K. pneumoniae* MGH78578-adjacent ORFs were *marR* (encodes a putative regulatory protein) and KPN_03281 and KPN_03274 (encode hypothetical proteins). Sequence information outside the *mrk* cluster is not known for *K. pneumoniae* IA565. Arrows indicate the direction of transcription for each gene.

identical (771/781 nucleotides) to the region spanning nucleotides 3116637 to 3117411 of the *K. pneumoniae* MGH78578 genome. This region contains genes encoding a putative IS*1* transposase (KPN_02838) and an insertion element protein (KPN_02839). Further upstream we identified two putative ORFs (c4509 and c4510) that are highly similar to hypothetical genes found on the UPEC CFT073 chromosome (this region shares 96% [2010 of 2081] nucleotide sequence similarity with the corresponding region from CFT073). Downstream of *mrkF*, we identified an ORF (*orf1*) that encodes a putative cytoplasmic protein from *Salmonella enterica* SC-B67 (93% [296 of 315] nucleotide sequence similarity). The *mrk* gene cluster from *E. coli* MS2027 has an overall G+C content of 56.6%, which is closer to that found in *K. pneumoniae* MGH78578 (57.5%) than to that found in *E. coli* K-12 (50.8%). The nucleotide sequence similarity of each *mrk* gene (and the amino acid identity of its product) to the corresponding sequence from *K. pneumoniae* pIA565 (gb M55912) and *K. pneumoniae* MGH78578 (gb CP000647) is shown in Table 4.

***The mrk* locus promotes biofilm formation.** The *mrk* locus was amplified by PCR from *E. coli* MS2027 and cloned into the EcoRV site of pBR322 to generate plasmid pCO12. When this plasmid was introduced into *E. coli* MS528 (an MG1655 *fim flu* strain deficient in biofilm formation), we observed strong biofilm growth (Fig. 4). Biofilm formation was observed in static and dynamic growth conditions in M9 minimal medium (but not in LB broth). Plasmid pCO12 was also transformed into the three Tn*5* mutants deficient in biofilm formation. The introduction of pCO12 into these strains restored their ability to form biofilms (Fig. 4), which was also confirmed by SEM (Fig. 2E).

TABLE 4. Comparison of the *E. coli* MS2027 Mrk protein and nucleotide sequences with the corresponding sequences from *K. pneumoniae* IA565(pIA565) and *K. pneumoniae* MGH78578

Mrk protein	Putative function	% Amino acid identity (nucleotide sequence conservation) of indicated protein in *K. pneumoniae* strain	
		IA565 plasmid-encoded Mrk	MGH78578 chromosome-encoded Mrk
MrkA	Major subunit	90 (86)	94 (99)
MrkB	Chaperone	91 (83)	100 (99)
MrkC	Usher	87 (82)	99 (99)
MrkD	Adhesin	54 (81)	97 (98)
MrkF	Anchor	78 (76)	99 (99)

We next employed a continuous flow chamber system to examine the ability of type 3 fimbriae to promote biofilm formation by *E. coli* in dynamic conditions. Consistent with the results of our microtiter plate biofilm assays, *E. coli* MS2027 produced a strong biofilm (with a depth of approximately 10 μm), while *E. coli* MS2003 (*mrkD*::Tn*5*) was unable to form a biofilm (Fig. 5). The defect in biofilm growth by *E. coli* MS2003 could be complemented by the addition of plasmid pCO12 (which contains the *mrk* gene cluster from *E. coli* MS2027). Thus, type 3 fimbriae can promote strong biofilm growth by *E. coli* in two distinct in vitro model systems.

Type 3 fimbrial expression is not associated with colonization of the mouse urinary tract. *E. coli* MS2027 and the *mrkD* mutant MS1486 were tested for their ability to colonize and survive in the mouse urinary tract. We did not observe any significant difference in the ability of either strain to colonize the mouse bladder following transurethral infection. We also tested these two strains in a competition challenge experiment using a 50:50 mixture of each strain as the inoculum. However, no difference in colonization of the bladder was observed (data not shown). Neither strain was isolated from the mouse kidney at the time points assayed.

Distribution of *mrk* genes in UPEC and other UTI pathogens. The finding that the *mrk* genes were located on a conjugative plasmid in *E. coli* prompted us to test for the prevalence of these genes in UPEC and other CAUTI pathogens. Primers were designed to PCR amplify an internal segment of the *mrkB* gene. First we tested for the presence of *mrkB* in the remaining 64 CAUTI *E. coli* strains from our collection. Two of these strains had positive PCR results and were confirmed by DNA

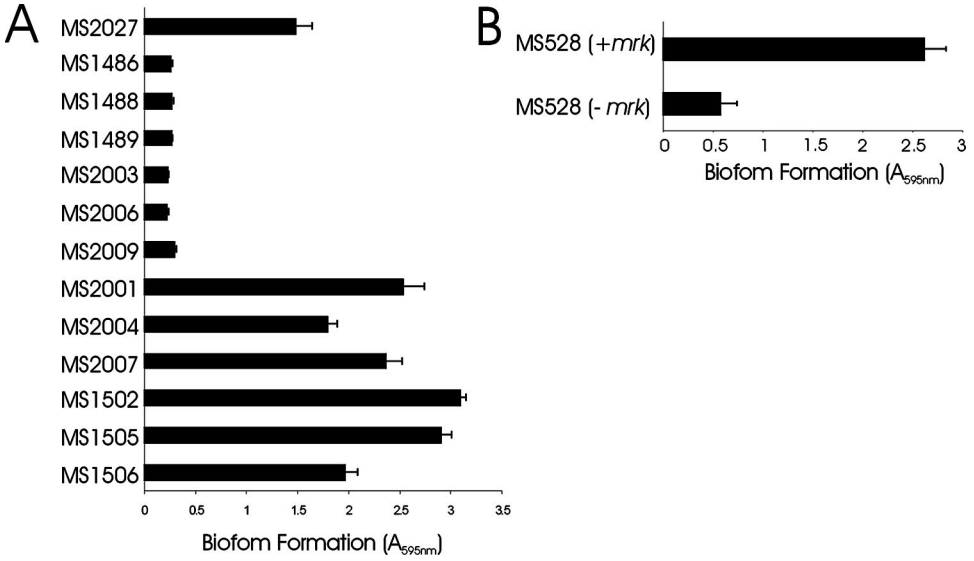

FIG. 4. (A) Biofilm formation by *E. coli* MS2027 and derivatives. Strains were grown at 37°C in PVC microtiter plates containing M9 medium (supplemented with 0.2% glucose) for 16 h under shaking conditions, washed to remove unbound cells, and stained with 0.1% crystal violet. Biofilm formation was quantified by resuspending adhered cells in ethanol-acetate (80:20) and measuring the absorbance at 595 nm. The results are presented as the average of eight individual replicates (± standard deviation). Shown are the results for MS1486 (MS2027 *mrkD*::Tn*5kan*), MS1488 (MS2027 *mrkB*::Tn*5kan*), MS1489 (MS2027 *mrkA*::Tn*5kan*), MS2003, MS2006, and MS2009, *mrk* mutants containing pBR322; MS2001, MS2004, and MS2007, *mrk* mutants containing pCO12 (*mrk*$^+$); MS1502 (*rmlC* mutant); MS1505 (*manB* mutant); and MS1506 (*kpsM* mutant). (B) Biofilm formation by *E. coli* MS528 and *E. coli* MS528 containing pCO12. Cells were grown and analyzed for biofilm formation as described above. The introduction of plasmid pCO12 (containing the *mrk* gene cluster from MS2027) into MS528 promoted strong biofilm growth. −, absence of; +, presence of.

sequencing. Next, we tested for the presence of *mrkB* in 70 CAUTI pathogens representing different gram-negative organisms isolated from UTI patients from the same location (Table 5). The *mrk* genes were detected from *K. pneumoniae*, *K. oxytoca*, *C. koseri*, and *C. freundii* CAUTI isolates (Table 5). The identity of each PCR product was confirmed by DNA sequencing. To determine whether the presence of the *mrk* genes was specific to CAUTI strains, we also tested for their prevalence in 45 *E. coli* strains isolated from cystitis and pyelonephritis patients. Among these strains, 2 of 45 contained the *mrkB* gene as determined by PCR amplification and DNA sequencing. Finally, we tested for the prevalence of *mrkB* in strains from the ECOR collection; three strains had positive PCR products for these genes, with results confirmed as correct by DNA sequencing. All of the organisms that contained the *mrkB* gene displayed a positive MR/K agglutination phenotype following growth in M9 minimal medium. We note that the *C. koseri* and *C. freundii* strains required growth in M9

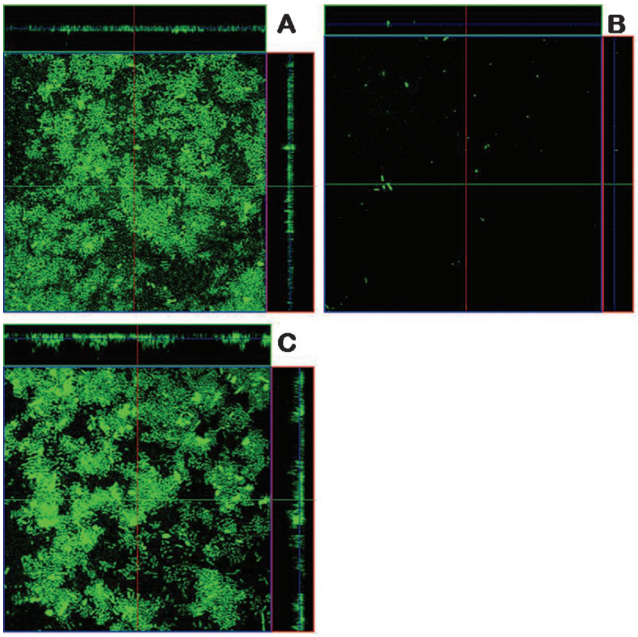

FIG. 5. Flow chamber biofilm formation of *E. coli* MS2027 (A), *E. coli* MS2003 (B), and *E. coli* MS2001 (C). Biofilm development was monitored by confocal scanning laser microscopy 24 h after inoculation. Micrographs represent horizontal sections. Depicted to the right and below are vertical sections through the biofilm collected at the positions indicated by the lines.

TABLE 5. Prevalence of *mrkB* gene and MR/K agglutination phenotype among UTI strains

Bacterial species and strain type	Total no. of strains	Presence[a] of:	
		mrkB	MR/K HA
Escherichia coli			
CAUTI	93	3 (3.2)	3 (3.2)
ABU	23	0 (0)	0 (0)
Cystitis	19	1 (5.3)	1 (5.3)
Pyelonephritis	26	1 (3.8)	1 (3.8)
ECOR	72	3 (4.2)	3 (4.2)
Other species			
C. freundii	7	1 (14.3)	1 (14.3)
C. koseri	9	9 (100)	9 (100)
K. oxytoca	2	2 (100)	2 (100)
K. pneumoniae	15	13 (86.7)	13 (86.7)

[a] Values are shown as no. (%).

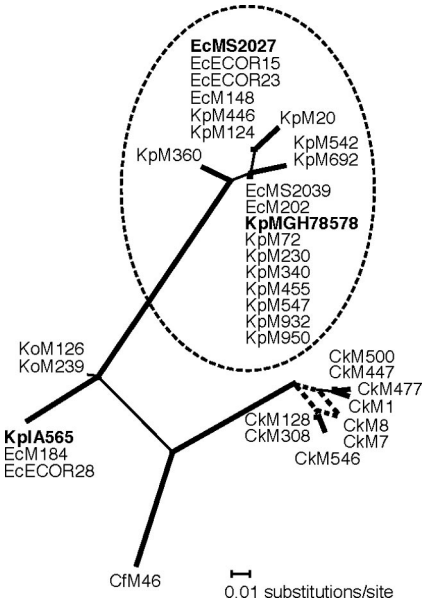

FIG. 6. Unrooted phylogram of type 3 family chaperone genes (*mrkB*). Branch confidence levels are indicated by line thickness: thick, >90%; thin, >50%; dashed, <50%. Confidence levels were determined from 1,000 bootstrap replicates of DNA maximum likelihood trees prepared by using PHYLIP DNAML (8, 12, 16, 20). A network of all 1,000 trees was prepared by using the consensus network method (8, 12, 16, 20), as implemented by SplitsTree, version 4 (8, 12, 16, 20). Taxon IDs include species name abbreviations as suffixes (Ec, *E. coli*; Cf, *C. freundii*; Ck, *C. koseri*; Ko, *K. oxytoca*; and Kp, *K. pneumoniae*), followed by a unique strain identifier. The major group containing *E. coli* MS2027 and *K. pneumoniae* MGH78578 (shown in bold) is circled for greater clarity. *K. pneumoniae* IA565 is also shown in bold.

minimal medium for 72 h under static conditions to induce MR/K agglutination.

Comparison of *mrkB* DNA sequences from different UTI pathogens. An unrooted maximum likelihood DNA phylogram was constructed from 36 aligned *mrkB* gene fragments (130 nucleotides in length, comprising 35 polymorphic sites, 28 of which were informative). A consensus network tree of 1,000 bootstrap replicates revealed five distinct groups, ranging from 20 members (represented by *K. pneumoniae* MG78758) to one member (*C. freundii*) (Fig. 6). The most common primary allele is found in both *E. coli* and *K. pneumoniae* (e.g., *E. coli* MS2039 and *Klebsiella pneumoniae* MGH78578 *mrkB* sequences are identical). Furthermore, two *E. coli mrkB* sequences (M184 and ECOR28) are identical to the plasmid-borne *Klebsiella pneumoniae* pIA565 *mrkB*, which shares only 85% nucleotide identity with *mrkB* from strain MGH78578. These observations strongly suggest lateral gene transfer of *mrkB* in *E. coli* and *K. pneumoniae*. Comparisons of full-length *mrkA* and *mrkC* sequences from *K. pneumoniae* IA565 and MGH78578 with *E. coli* MS2027 show similar levels of divergence to that observed for *mrkB* (Table 4). This result suggests that the *mrkB* phylogenetic tree is representative of *mrkA* and *mrkC* and that en bloc transfer of the *mrk* cluster has occurred.

The long internal branches represent the divergence of primary *mrkB* alleles (Fig. 6), with an average interallelic nucleotide diversity of 9.8%. Secondary variant types are observed only within the KpMGH78578 and *C. koseri* groups (1% and 1.8% intra-allelic nucleotide diversity, respectively). No statistically significant evidence of recombination was detected between groups according to the pairwise homoplasy index test (8, 12, 16, 20). According to the consensus network (Fig. 6), there is some incompatibility in the divergence of *C. koseri* clones (as indicated by more than one branch leading to the CkM7/CkM8 tip); however, there are too few informative sites ($n = 3$) to accurately discriminate recombination from recurrent mutation among this group. Tree topologies very similar to those obtained by using DNA maximum likelihood were obtained by using parsimony- and distance-based phylogenetic methods (data not shown).

DISCUSSION

CAUTI is associated with biofilm formation on the inner surfaces of indwelling catheters. *E. coli* is a major cause of CAUTI, and several surface factors that contribute to biofilm growth by *E. coli* have been characterized. Type 1 fimbria expression is associated with persistence in the long-term-catheterized urinary tract (29), and minor modifications in the FimH adhesin can enhance biofilm formation (45). Flagella are motility organelles that play a role in the initial adhesion phase of biofilm formation (36). Curli are thin aggregative fibers involved in bacterial attachment and biofilm formation (38). In many *E. coli* strains, the expression of curli is temperature sensitive and occurs at 28°C but not at 37°C. Antigen 43 (Ag43) is a self-recognizing autotransporter adhesin that is associated with cell aggregation, biofilm formation, and urovirulence (6, 24, 54). Other factors that promote biofilm growth by *E. coli* include conjugative pili (14, 37) and several recently described cryptic autotransporter proteins (39). In this study, we have demonstrated that genes involved in capsule synthesis, O antigen production, and type 3 fimbriae influence biofilm formation by the CAUTI *E. coli* strain MS2027.

Three Tn*5* mutants of *E. coli* MS2027 that possessed an increased biofilm formation phenotype were identified. The Tn*5* insertions resulted in the disruption of genes associated with O antigen synthesis (*rmlC* and *manB*) and capsule synthesis (*kpsM*). Capsular polysaccharides are produced by many uropathogenic bacteria and provide protection from host cell phagocytosis. Capsular polysaccharides also contribute to UPEC biofilm formation in the bladder (6, 11). The enhanced biofilm growth of *E. coli* MS1506 might at first sight appear contradictory to these comments. However, our observations may reflect the limitations of the microtiter plate biofilm assay in comparison to in vivo biofilm growth. *E. coli* MS1506 contained a Tn*5* insertion in the *kpsM* gene, which encodes an integral membrane protein involved in the translocation of the polysialic capsule. Previous studies have shown that an *E. coli kpsM* mutant is defective in capsule synthesis (35). While we have not shown that MS1506 is defective in capsule production, it is tempting to speculate that its enhanced biofilm growth is associated with the unmasking of other adhesins. In support of this hypothesis, a recent study reported that the expression of the nonfimbrial adhesin Ag43 in unencapsulated *Klebsiella* strains results in enhanced biofilm growth compared to capsulated strains that express Ag43, suggesting that the capsule might block the activity of other surface-located adhesins (43). The capsule shielding effect has also been demon-

strated in adherence studies of other organisms, including *E. coli* (40, 43), *Neisseria meningitidis* (56), and *Haemophilus influenzae* (50). Furthermore, the function of type 1 fimbriae has been shown to be impeded by the presence of a capsule on the bacterial cell surface (42) and thus reduced capsule synthesis by *E. coli* MS1506 may enhance the contribution of fimbriae to biofilm formation. We note that soluble polysaccharide secreted by UPEC strains that produce a group II capsule was recently shown to inhibit biofilm growth by preventing adhesion (55). Therefore, we cannot rule out the possibility that the enhanced biofilm growth of MS1506 is due to reduced secretion of antiadhesive polysaccharide material. The enhanced biofilm growth by *E. coli* MS1508 and *E. coli* MS1509 might be associated with a similar mechanism, since many UPEC strains are known to produce large O antigen structures. We are currently attempting to elucidate the role of the capsule and O antigen in UPEC colonization and biofilm formation in an in vivo model of CAUTI.

The decreased biofilm growth by Tn*5* mutants of *E. coli* MS2027 was due to the disruption of genes encoding type 3 fimbriae. Three biofilm-deficient mutants were identified, all of which contained a Tn*5* insertion in the *mrk* operon. The role of type 3 fimbriae in biofilm formation was confirmed by the complementation of each of these mutants with a plasmid (pCO12) containing the *mrk* genes. Type 3 fimbriae are thin, filamentous structures (4 to 5 nm wide and 0.5 to 2 μm long) that extend from the surface of the cell (10) and are morphologically similar to K88 and K99 fimbriae (26). Type 3 fimbriae are characterized by their ability to mediate MR agglutination of tannic acid-treated RBC (which is referred to as MR *Klebsiella*-like or MR/K agglutination) (26). MR/K agglutination is conferred by the MrkD adhesin (5, 19). MrkD also mediates binding to the basolateral surface of renal tubular, tracheal, and bronchial cells via a high-affinity interaction with type V collagen (17, 51, 52). Type 3 fimbriae from *K. pneumoniae* have also been shown to mediate biofilm formation (21).

Type 3 fimbriae are most commonly associated with *Klebsiella* spp. (13). However, they are also produced by other members of the *Enterobacteriaceae* family, including *Enterobacter*, *Morganella*, *Proteus*, *Providencia*, *Serratia*, *Salmonella*, and *Yersinia* species (1–4, 13, 30–33, 48). Here we demonstrate that type 3 fimbriae are also produced by *E. coli*, *C. koseri*, and *C. freundii*. In *E. coli* MS2027, the *mrk* genes are located on a conjugative plasmid of approximately 45 kb (C.-L. Y. Ong, A. G. McEwan, and M. A. Schembri, unpublished data). Plasmid-carried *mrk* genes have previously been identified for *K. pneumoniae* and *Y. enterocolitica* (5, 13). *K. pneumoniae* IA565 possesses both chromosomal and plasmid-carried *mrk* genes; the plasmid pIA565 contains a functional copy of *mrkA* and *mrkD*, while only *mrkA* has been detected on the *K. pneumoniae* IA565 chromosome. The *mrk* genes from pIA565 have been well characterized and possess the same genetic arrangement as do the *mrk* genes on plasmid pMS2027. However, the sequence upstream of *mrkA* is different between the two gene clusters (the sequence downstream of *mrkF* on pIA565 has not been reported). On plasmid pIA565, a gene (*mrkE*) encoding a putative regulator protein is located immediately upstream of *mrkA* (5). This gene is not present on pMS2027. Instead, we identified a putative transposase-encoding gene upstream of *mrkA* and the entire cluster is flanked by two putative insertion sequence elements. Thus, it seems likely that the *mrk* cluster on plasmid pMS2027 is associated with a mobile genetic element. Importantly, the presence of *mrk* genes in *E. coli* was not unique to strains in our UTI collection, as three strains from the ECOR collection also contained *mrkABC* and caused MR/K hemagglutination. The location of the *mrk* genes from these strains remains to be determined.

We observed that the expression of type 3 fimbriae was dependent on the growth medium. *E. coli* MS2027 produced a strong biofilm and caused characteristic MR/K agglutination when grown in M9 minimal medium supplemented with glucose but not when grown in LB medium. This finding is consistent with the results of previous reports of type 3 fimbria expression in *K. pneumoniae*, where bacteria grown in minimal medium in the presence of glycerol or glucose resulted in a stronger MR/K hemagglutination reaction than did bacteria grown in complex medium (18, 47). This result suggests a similar method of regulation of the type 3 fimbrial genes of *K. pneumoniae* IA565 and *E. coli* MS2027, despite the absence of the putative *mrkE* regulator gene on pMS2027. It is interesting that all of the *mrkABC*-positive strains identified in this study caused MR/K agglutination, since previous studies have shown that not all *Klebsiella* spp. possess the adhesin-encoding *mrkD* gene (19).

We compared the *mrk* cluster from *E. coli* MS2027 with the *mrk* clusters from *K. pneumoniae* MGH78578 and pIA565 (Table 4). All five *mrkABCDE* genes showed remarkable sequence similarity to the chromosomally located MGH78578 sequences (98.8% ± 0.4%) compared to that shown by the respective pIA565 sequences (81.6% ± 3.6%). The presence of insertion sequences adjacent to the plasmid-borne *E. coli* MS2027 *mrk* cluster and the G+C content suggest that there was relatively recent lateral transfer from a *K. pneumoniae* strain, although we cannot rule out the possibility that both strains acquired the cluster independently from a third species. To assess the distribution of this cluster among UTI organisms, we amplified and sequenced a fragment of the chaperone gene (*mrkB*), which is typically the most highly conserved gene within chaperone/usher fimbrial clusters. Phylogenetic analyses indicated there were five primary alleles which, with the exception of the two *K. oxytoca* strains, are strongly supported by long internal branches (Fig. 6). The most common allele is that shared by *K. pneumoniae* MGH78578 and *E. coli* MS2027. This allele is also shared by *E. coli* CAUTI strains MS2039 and M148 and cystitis strain M202. Interestingly, *mrkB* from the pyelonephritis *E. coli* strain M184 is identical to that found in *K. pneumoniae* pIA565. The observation that two alleles (represented by strains MGH78578 and IA565) contain sequences that are identical in both *E. coli* and *K. pneumoniae* species, but substantially divergent from each other, is strong evidence of recurrent and recent lateral gene transfer of the *mrk* cluster among *K. pneumoniae* and *E. coli* UTI strains.

In conclusion, we have identified the capsule, O antigen, and type 3 fimbriae as factors that affect biofilm growth by CAUTI *E. coli*. Type 3 fimbriae are produced by many members of the *Enterobacteriaceae* family that are associated with opportunistic infections. Biofilm growth mediated by type 3 fimbriae may be important for the survival of these organisms on the surfaces of urinary catheters and within the hospital environment. We speculate that the *mrk* gene cluster in *E. coli* MS2027 may

have originated from *K. pneumoniae*, and we are currently investigating this possibility.

ACKNOWLEDGMENTS

This work was supported by grants from the National Health and Medical Research Council (NHMRC) of Australia (grant no. 455914) and the Australian Research Council (grant no. DP0666852). C.-L.Y.O. was supported by an International Postgraduate Research Scholarship from the University of Queensland. S.A.B. was supported by an NHRMC Howard Florey Centenary fellowship.

The *K. pneumoniae* genome sequence data were produced by the Genome Sequencing Center at the Washington University School of Medicine in St. Louis, MO.

REFERENCES

1. **Adegbola, R. A., and D. C. Old.** 1985. Fimbrial and non-fimbrial hemagglutinins in enterobacter-aerogenes. J. Med. Microbiol. **19:**35–43.
2. **Adegbola, R. A., and D. C. Old.** 1983. Fimbrial hemagglutinins in enterobacter species. J. Gen. Microbiol. **129:**2175–2180.
3. **Adegbola, R. A., and D. C. Old.** 1982. New fimbrial hemagglutinin in *Serratia* species. Infect. Immun. **38:**306–315.
4. **Adegbola, R. A., D. C. Old, and S. Aleksic.** 1983. Rare Mr/K-like hemagglutinins (and type-3-like fimbriae) of salmonella strains. FEMS Microbiol. Lett. **19:**233–238.
5. **Allen, B. L., G. F. Gerlach, and S. Clegg.** 1991. Nucleotide sequence and functions of *mrk* determinants necessary for expression of type 3 fimbriae in *Klebsiella pneumoniae*. J. Bacteriol. **173:**916–920.
6. **Anderson, G. G., J. J. Palermo, J. D. Schilling, R. Roth, J. Heuser, and S. J. Hultgren.** 2003. Intracellular bacterial biofilm-like pods in urinary tract infections. Science **301:**105–107.
7. **Blaesing, F., A. Muhlenweg, S. Vierling, G. Ziegelin, S. Pelzer, and E. Lanka.** 2005. Introduction of DNA into Actinomycetes by bacterial conjugation from E-coli—an evaluation of various transfer systems. J. Biotechnol. **120:** 146–161.
8. **Bruen, T. C., H. Philippe, and D. Bryant.** 2006. A simple and robust statistical test for detecting the presence of recombination. Genetics **172:**2665–2681.
9. **Delorenzo, V., M. Herrero, U. Jakubzik, and K. N. Timmis.** 1990. Mini-Tn*5* transposon derivatives for insertion mutagenesis, promoter probing, and chromosomal insertion of cloned DNA in gram-negative eubacteria. J. Bacteriol. **172:**6568–6572.
10. **Duguid, J. P.** 1959. Fimbriae and adhesive properties in Klebsiella strains. J. Gen. Microbiol. **21:**271–286.
11. **Eto, D. S., J. L. Sundsbak, and M. A. Mulvey.** 2006. Actin-gated intracellular growth and resurgence of uropathogenic *Escherichia coli*. Cell. Microbiol. **8:**704–717.
12. **Felsenstein, J.** 2004. PHYLIP (phylogeny inference package), version 3.6. Department of Genome Sciences, Seattle, WA.
13. **Gerlach, G. F., B. L. Allen, and S. Clegg.** 1989. Type 3 fimbriae among enterobacteria and the ability of spermidine to inhibit Mr/K hemagglutination. Infect. Immun. **57:**219–224.
14. **Ghigo, J. M.** 2001. Natural conjugative plasmids induce bacterial biofilm development. Nature **412:**442–445.
15. **Hagberg, L., U. Jodal, T. K. Korhonen, G. Lidin-Janson, U. Lindberg, and C. Svanborg Eden.** 1981. Adhesion, hemagglutination, and virulence of *Escherichia coli* causing urinary tract infections. Infect. Immun. **31:**564–570.
16. **Holland, B., and V. Moulton.** 2003. Consensus networks: a method for visualizing incompatibilities in collections of trees, p. 165–176. *In* G. Benson and R. Page (ed.), Algorithms in bioinformatics, WABI 2003. Springer-Verlag, Berlin, Germany.
17. **Hornick, D. B., B. L. Allen, M. A. Horn, and S. Clegg.** 1992. Adherence to respiratory epithelia by recombinant *Escherichia coli* expressing *Klebsiella pneumoniae* type 3 fimbrial gene products. Infect. Immun. **60:**1577–1588.
18. **Hornick, D. B., B. L. Allen, M. A. Horn, and S. Clegg.** 1991. Fimbrial types among respiratory isolates belonging to the family *Enterobacteriaceae*. J. Clin. Microbiol. **29:**1795–1800.
19. **Hornick, D. B., J. Thommandru, W. Smits, and S. Clegg.** 1995. Adherence properties of an *mrkD*-negative mutant of *Klebsiella pneumoniae*. Infect. Immun. **63:**2026–2032.
20. **Huson, D. H., and D. Bryant.** 2006. Application of phylogenetic networks in evolutionary studies. Mol. Biol. Evol. **23:**254–267.
21. **Jagnow, J., and S. Clegg.** 2003. Klebsiella pneumoniae MrkD-mediated biofilm formation on extracellular matrix- and collagen-coated surfaces. Microbiology **149:**2397–2405.
22. **Kallenius, G., R. Mollby, S. B. Svenson, I. Helin, H. Hultberg, B. Cedergren, and J. Winberg.** 1981. Occurrence of P-fimbriated *Escherichia coli* in urinary tract infections. Lancet **ii:**1369–1372.
23. **Kjaergaard, K., M. A. Schembri, C. Ramos, S. Molin, and P. Klemm.** 2000. Antigen 43 facilitates formation of multispecies biofilms. Environ. Microbiol. **2:**695–702.
24. **Klemm, P., L. Hjerrild, M. Gjermansen, and M. A. Schembri.** 2004. Structure-function analysis of the self-recognizing antigen 43 autotransporter protein from Escherichia coli. Mol. Microbiol. **51:**283–296.
25. **Klemm, P., and M. A. Schembri.** 2000. Bacterial adhesins: function and structure. Int. J. Med. Microbiol. **290:**27–35.
26. **Korhonen, T. K., E. Tarkka, H. Ranta, and K. Haahtela.** 1983. Type 3 fimbriae of *Klebsiella* sp.: molecular characterization and role in bacterial adhesion to plant roots. J. Bacteriol. **155:**860–865.
27. **Leffler, H., and C. Svanborg-Eden.** 1981. Glycolipid receptors for uropathogenic *Escherichia coli* on human erythrocytes and uroepithelial cells. Infect. Immun. **34:**920–929.
28. **Mahapatra, N. R., S. Ghosh, P. K. Sarkar, and P. C. Banerjee.** 2003. Generation of novel plasmids in Escherichia coli S17-1(pSUP106). Curr. Microbiol. **46:**318–323.
29. **Mobley, H. L., G. R. Chippendale, J. H. Tenney, R. A. Hull, and J. W. Warren.** 1987. Expression of type 1 fimbriae may be required for persistence of *Escherichia coli* in the catheterized urinary tract. J. Clin. Microbiol. **25:** 2253–2257.
30. **Old, D. C., and R. A. Adegbola.** 1985. Antigenic relationships among type-3 fimbriae of Enterobacteriaceae revealed by immunoelectronmicroscopy. J. Med. Microbiol. **20:**113–121.
31. **Old, D. C., and R. A. Adegbola.** 1982. Hemagglutinins and fimbriae of Morganella, Proteus and Providencia. J. Med. Microbiol. **15:**551–564.
32. **Old, D. C., and R. A. Adegbola.** 1984. Relationships among broad-spectrum and narrow-spectrum mannose-resistant fimbrial hemagglutinins in different Yersinia species. Microbiol. Immunol. **28:**1303–1311.
33. **Old, D. C., and S. S. Scott.** 1981. Hemagglutinins and fimbriae of *Providencia* spp. J. Bacteriol. **146:**404–408.
34. **Paterson, D. L., and J. Lipman.** 2007. Returning to the pre-antibiotic era in the critically ill: the XDR problem. Crit. Care Med. **35:**1789–1791.
35. **Pigeon, R. P., and R. P. Silver.** 1997. Analysis of the G93E mutant allele of KpsM, the membrane component of an ABC transporter involved in polysialic acid translocation in Escherichia coli K1. FEMS Microbiol. Lett. **156:** 217–222.
36. **Pratt, L. A., and R. Kolter.** 1998. Genetic analysis of Escherichia coli biofilm formation: roles of flagella, motility, chemotaxis and type I pili. Mol. Microbiol. **30:**285–293.

36a. **R Development Core Team.** 2007. R: a language and environment for statistical computing. R Foundation for Statistical Computing, Vienna, Austria.

37. **Reisner, A., J. A. Haagensen, M. A. Schembri, E. L. Zechner, and S. Molin.** 2003. Development and maturation of Escherichia coli K-12 biofilms. Mol. Microbiol. **48:**933–946.
38. **Römling, U.** 2005. Characterization of the rdar morphotype, a multicellular behaviour in Enterobacteriaceae. Cell. Mol. Life Sci. **62:**1234–1246.
39. **Roux, A., C. Beloin, and J. M. Ghigo.** 2005. Combined inactivation and expression strategy to study gene function under physiological conditions: application to identification of new *Escherichia coli* adhesins. J. Bacteriol. **187:**1001–1013.
40. **Runnels, P. L., and H. W. Moon.** 1984. Capsule reduces adherence of enterotoxigenic *Escherichia coli* to isolated intestinal epithelial cells of pigs. Infect. Immun. **45:**737–740.
41. **Sambrook, J., and D. W. Russell.** 2001. Molecular cloning: a laboratory manual, 3rd ed., vol. 1. Cold Spring Harbor Laboratory Press, Cold Spring Harbor, NY.
42. **Schembri, M. A., J. Blom, K. A. Krogfelt, and P. Klemm.** 2005. Capsule and fimbria interaction in *Klebsiella pneumoniae*. Infect. Immun. **73:**4626–4633.
43. **Schembri, M. A., D. Dalsgaard, and P. Klemm.** 2004. Capsule shields the function of short bacterial adhesins. J. Bacteriol. **186:**1249–1257.
44. **Schembri, M. A., K. Kjaergaard, and P. Klemm.** 2003. Global gene expression in Escherichia coli biofilms. Mol. Microbiol. **48:**253–267.
45. **Schembri, M. A., and P. Klemm.** 2001. Biofilm formation in a hydrodynamic environment by novel FimH variants and ramifications for virulence. Infect. Immun. **69:**1322–1328.
46. **Schembri, M. A., E. V. Sokurenko, and P. Klemm.** 2000. Functional flexibility of the FimH adhesin: insights from a random mutant library. Infect. Immun. **68:**2638–2646.
47. **Schurtz, T. A., D. B. Hornick, T. K. Korhonen, and S. Clegg.** 1994. The type 3 fimbrial adhesin gene (*mrkD*) of *Klebsiella* species is not conserved among all fimbriate strains. Infect. Immun. **62:**4186–4191.
48. **Sebghati, T. A. S., T. K. Korhonen, D. B. Hornick, and S. Clegg.** 1998. Characterization of the type 3 fimbrial adhesins of *Klebsiella* strains. Infect. Immun. **66:**2887–2894.
49. **Stamm, W. E.** 1991. Catheter-associated urinary tract infections: epidemiology, pathogenesis, and prevention. Am. J. Med. **91:**65S–71S.
50. **St. Geme, J. W., III, and S. Falkow.** 1991. Loss of capsule expression by *Haemophilus influenzae* type b results in enhanced adherence to and invasion of human cells. Infect. Immun. **59:**1325–1333.
51. **Tarkkanen, A. M., B. L. Allen, B. Westerlund, H. Holthofer, P. Kuusela, L. Risteli, S. Clegg, and T. K. Korhonen.** 1990. Type V collagen as the target for

type-3 fimbriae, enterobacterial adherence organelles. Mol. Microbiol. **4:**1353–1361.
52. **Tarkkanen, A. M., R. Virkola, S. Clegg, and T. K. Korhonen.** 1997. Binding of the type 3 fimbriae of *Klebsiella pneumoniae* to human endothelial and urinary bladder cells. Infect. Immun. **65:**1546–1549.
53. **Ulett, G. C., A. N. Mabbett, K. C. Fung, R. I. Webb, and M. A. Schembri.** 2007. The role of F9 fimbriae of uropathogenic Escherichia coli in biofilm formation. Microbiology **153:**2321–2331.
54. **Ulett, G. C., J. Valle, C. Beloin, O. Sherlock, J. M. Ghigo, and M. A. Schembri.** 2007. Functional analysis of antigen 43 in uropathogenic *Escherichia coli* reveals a role in long-term persistence in the urinary tract. Infect. Immun. **75:**3233–3244.
55. **Valle, J., S. Da Re, N. Henry, T. Fontaine, D. Balestrino, P. Latour-Lambert, and J. M. Ghigo.** 2006. Broad-spectrum biofilm inhibition by a secreted bacterial polysaccharide. Proc. Natl. Acad. Sci. USA **103:**12558–12563.
56. **Virji, M., K. Makepeace, D. J. Ferguson, M. Achtman, and E. R. Moxon.** 1993. Meningococcal Opa and Opc proteins: their role in colonization and invasion of human epithelial and endothelial cells. Mol. Microbiol. **10:**499–510.
57. **Vrionis, H. A., A. J. Daugulis, and A. M. Kropinski.** 2002. Identification and characterization of the AgmR regulator of *Pseudomonas putida*: role in alcohol utilization. Appl. Microbiol. Biotechnol. **58:**469–475.
58. **Warren, J. W.** 2001. Catheter-associated urinary tract infections. Int. J. Antimicrob. Agents **17:**299–303.
59. **Warren, J. W., D. Damron, J. H. Tenney, J. M. Hoopes, B. Deforge, and H. L. Muncie, Jr.** 1987. Fever, bacteremia, and death as complications of bacteriuria in women with long-term urethral catheters. J. Infect. Dis. **155:**1151–1158.
60. **Warren, J. W., J. H. Tenney, J. M. Hoopes, H. L. Muncie, and W. C. Anthony.** 1982. A prospective microbiologic study of bacteriuria in patients with chronic indwelling urethral catheters. J. Infect. Dis. **146:**719–723.
61. **Watson, N.** 1988. A new revision of the sequence of plasmid pBR322. Gene **70:**399–403.
62. **Wu, X. R., T. T. Sun, and J. J. Medina.** 1996. In vitro binding of type 1-fimbriated *Escherichia coli* to uroplakins Ia and Ib: relation to urinary tract infections. Proc. Natl. Acad. Sci. USA **93:**9630–9635.
63. **Zogaj, X., M. Nimtz, M. Rohde, W. Bokranz, and U. Romling.** 2001. The multicellular morphotypes of Salmonella typhimurium and Escherichia coli produce cellulose as the second component of the extracellular matrix. Mol. Microbiol. **39:**1452–1463.